Structure and phase equilibria of microemulsions

David Andelman, M. E. Cates, D. Roux, and S. A. Safran

Citation: J. Chem. Phys. **87**, 7229 (1987); doi: 10.1063/1.453367
View online: http://dx.doi.org/10.1063/1.453367
View Table of Contents: http://jcp.aip.org/resource/1/JCPSA6/v87/i12
Published by the American Institute of Physics.

Structure and phase equilibria of microemulsions

David Andelman,[a] M. E. Cates,[b] D. Roux,[c] and S. A. Safran
Corporate Research Science Laboratories, Exxon Research and Engineering Company, Annandale, New Jersey 08801

(Received 18 February 1987; accepted 3 September 1987)

We present a simple phenomenological model to describe the phase equilibria and structural properties of microemulsions. Space is divided into cells of side ξ; each cell is filled with either pure water or oil. Surfactant molecules are presumed to form an incompressible fluid monolayer at the oil–water interface. The monolayer is characterized by a size-dependent bending constant $K(\xi)$, which is small for $\xi \geqslant \xi_K$, the de Gennes–Taupin persistence length. The model predicts a middle-phase microemulsion of structural length scale $\xi \approx \xi_K$ which coexists with dilute phases of surfactant in oil and surfactant in water. (These phases have $\xi \approx a$, a being a molecular length.) On the same ternary phase diagram, we find also two regions of two-phase equilibrium involving upper- and lower-phase microemulsions that coexist with either almost pure water or oil. At low temperatures and/or high values of the bare bending constant, $K_0 \equiv K(a)$, the middle-phase microemulsion may be entirely precluded by separation to a lamellar phase, whereas at high temperature and/or low values of K_0, there is a first-order transition between a disordered microemulsion and a lamellar phase. In the absence of spontaneous curvature the phase diagram is oil–water symmetric. It may be asymmetrized by: (i) spontaneous curvature in the middle phase or (ii) a difference between the free energy of the two dilute phases. If the asymmetry is sufficiently large, the three-phase region disappears.

I. INTRODUCTION

A. Microemulsions: A review

Microemulsions are thermodynamically stable, fluid, oil–water–surfactant mixtures.[1] The surfactant volume fraction is typically low ($\sim 5\%$); most microemulsions also contain cosurfactant (alcohol) and/or salt. A characteristic feature of microemulsions, as opposed to simple liquid mixtures, is that the oil and water remain separated in coherent domains, typically tens or hundreds of angstroms in size. Because of their amphiphilic character, the surfactant molecules prefer the interfacial environment to either that of water or oil. This results in an extensive oil–water interface.

The configuration of the oil and water domains varies with composition. For small fractions of oil in water or of water in oil, the structure is that of globules[2] whose colloidal properties are well understood.[3] However, when the volume fractions of oil and water are comparable, one expects random,[4] bicontinuous[5] structures to form.[6–8] Of course, under appropriate conditions (particularly when the volume-fraction of surfactant is higher than a few percent) various ordered structures, such as lamellae, cubic, or cylindrical structures, may also arise.[9]

A schematic series of ternary phase diagrams for a prototypical microemulsion system[10] is shown in Fig. 1. A characteristic feature is the presence of two- and three-phase regions on the phase diagram. In the two-phase regions there is coexistence between an almost pure phase (surfactant in oil or surfactant in water) and a microemulsion (lower or upper phase, respectively). In the three-phase region, a middle-

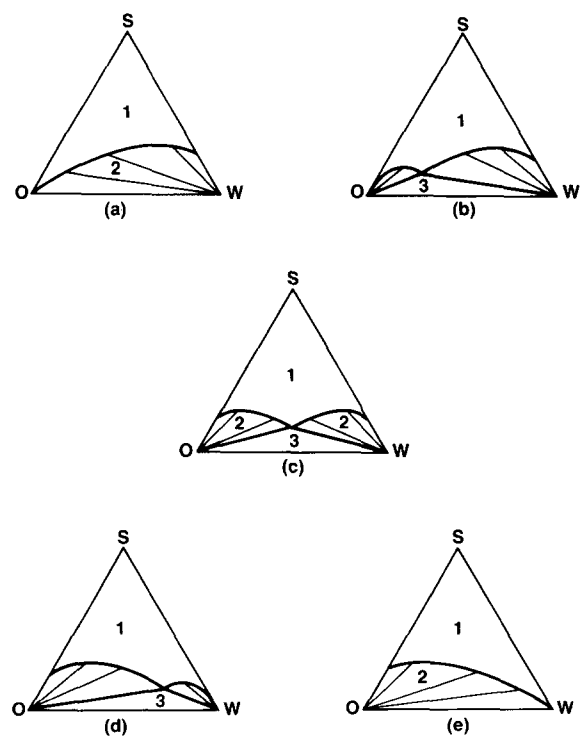

FIG. 1. Schematic phase diagrams for prototypical microemulsion systems. In (a) and (b) systems with asymmetry towards oil (thus coexisting with excess water) are shown. An oil–water symmetric system is shown in (c), and a system with asymmetry towards water is shown in (d) and (e). These triangular shaped phase diagrams are a convenient way to describe ternary systems. The corners of each triangle correspond to: pure surfactant (S), pure water (W), and pure oil (O). The numbers 1,2,3 indicate the number of coexisting phases and some of the tie lines are shown.

[a] Also at Laboratoire de Physique de la matière condensée, Collège de France, 75231 Paris Cedex 05, France. Permanent address: School of Physics and Astronomy, Tel Aviv University, Ramat-Aviv, 69978 Isreal.

[b] Present address: Institute for Theoretical Physics, University of California, Santa Barbara, CA 93106.

[c] Present address: Department of Chemistry, UCLA, Los Angeles, CA 90024. Permanent address: Centre Paul Pascal, CNRS, Domaine Universitaire, 33405, Talence Cedex France.

 0021-9606/87/247229-13$02.10

phase microemulsion coexists simultaneously with almost pure water and almost pure oil.[11]

In Fig. 1(c), the phase diagram is oil–water symmetric. This balance point is achieved under variation of a parameter such as salt concentration.[8] Such a parameter may be tuned so as to alter the spontaneous curvature of the surfactant film; it is commonly believed[3,12] that at the symmetric (balance) point there is no preferred direction of curvature [Fig. 1(c)]. In Figs. 1(a) and 1(b), there is spontaneous curvature toward oil (favoring globules of oil in water) and in Figs. 1(d) and 1(e) spontaneous curvature towards water (which favors globules of water in oil). Note that the three-phase region has entirely disappeared in Figs. 1(a) and 1(e). At the balance point, the middle-phase microemulsion shows ultralow interfacial tensions[13] ($\sigma \sim 10^{-3}$–10^{-5} dyn/cm) with both of the nearly pure phases with which it coexists; this results in a variety of technological applications, for example in chemically enhanced oil recovery.[14] Crudely one can argue that $\sigma \sim T/\xi^2$, where ξ is a structural length scale of order the domain size and T is the temperature. Thus, the observed ultralow interfacial tensions arise from the large ($\xi \sim 100$ Å) coherence lengths in these systems.

It should be emphasised that three-phase equilibrium as shown in Fig. 1 is usually obtained with the addition of alcohol, as well as salt.[15] Without alcohol, one normally sees instead ordered mesophases which preclude equilibria involving a middle phase microemulsion. It is thought that one effect of adding alcohol is to reduce the rigidity of the surfactant film.[16] This favors disordered microemulsion phases over ordered mesophases such as lamellae. (It certainly may also have an effect on the spontaneous curvature.)

There have so far been two differing approaches to the construction of thermodynamic models for microemulsions. In this paper we follow the "phenomenological" approach, which was initiated by Talmon and Prager,[4] and further developed by de Gennes and co-workers[16,17] and Widom.[18] In this approach one regards oil and water as continuum liquids; the interfacial surfactant layer is treated either as a flexible sheet, or in a microscopic manner similar to that of insoluble Langmuir monolayers.[19] The presence of salt and/or alcohol is not directly treated, but enters through the energy parameters of the interfacial sheet. The strategy is to fix the volume fractions of oil, water, and surfactant, and to then calculate the free energy of a hypothetical homogeneous phase of this composition. This generates a free energy as a function of composition, from which the phase diagram can be determined. In calculating the free energy, it is often convenient to describe the oil and water domains in terms of a coarse-grained lattice; in this procedure, the lattice spacing remains comparable to the domain size, which is usually much larger than a molecular length scale.

The second approach is based on the construction of "microscopic" lattice models, in which a cell of the lattice contains only a small number of molecules. This approach was initiated by Wheeler and Widom,[20] and has recently been extended by Widom[21] and others.[22] This microscopic approach, though of undoubted fundamental interest, may be more difficult to implement than the phenomenological one. In particular, a microscopic model of microemulsions must produce structural organization on a length scale (the domain size) much larger than that of the lattice.[23] It may, therefore, be argued that the microscopic approach is better suited to the description of long-range ordered mesophases, which occur at higher surfactant concentrations, than the description of random, bicontinuous structures, such as middle-phase microemulsions.[24]

B. Previous phenomenological models

As mentioned above, the first phenomenological model of disordered microemulsions was that of Talmon and Prager.[4] They considered a subdivision of space into random (Voronoi) polyhedra, which were filled at random with either oil or water, according to a probability proportional to the volume fraction of each component. The surfactant was presumed to form a monolayer at the interface between cells of water and oil; the area per surfactant molecule was taken as a fixed constant, $\Sigma = \Sigma_0$. The bending energy of the surfactant film was included (to some extent) by assuming the interface to be completely flat everywhere except at the edges of the Voronoi polyhedra, and assuming that the surfactant packing density is changed in the vicinity of the edges of the polyhedra. However, as already mentioned by Talmon and Prager, the energetics of this change are not explicitly included in the free energy. In addition, this does not take into account the harmonic curvature energy of the surfactant film used to model membranes and liquid crystals. A further discussion of the Talmon–Prager formulation may be found in Ref. 17. Despite these drawbacks, this model has proved very valuable as a starting point for improved phenomenological theories.

The first such improved theory was proposed by de Gennes and Taupin,[16] and studied in more detail by Jouffroy, Levinson, and de Gennes (JLG).[17] This model drew on a physical picture of undulating lamellae. By summing over undulation modes in a nearly flat sheet of bending constant K and zero surface tension, de Gennes and Taupin calculated a persistence length which may be defined by

$$\xi_K \approx a\, e^{4\pi K/\alpha T}. \tag{1.1}$$

Here α is a numerical constant, which is somewhat arbitrary. de Gennes and Taupin set $\alpha = 2$, but below we will find it convenient to use a different value ($\alpha = 1$). In any case, as discussed below, our results, when expressed in reduced units, are not sensitive to the exact value of α. However, since ξ_K depends exponentially on $K/\alpha T$, the phase diagram as a function of the unscaled volume fractions does depend on the values of K/T and α. In Eq. (1.1), a is a molecular size, which provides a lower cutoff in the wavelength of the undulations, and T is temperature (we set the Boltzmann constant, k_B equal to unity). The sheet remains flat over distances $\xi < \xi_K$ but is crumpled at larger length scales.

The JLG model simplified the Talmon–Prager one by dividing space into a lattice of cubes (rather than Voronoi polyhedra); the cubes are filled at random with oil or water according to their volume fractions. Based on the physical picture of the persistence length, they chose the lattice size to

be always equal to ξ_K. Within the random mixing approximation (to be explained in Sec. II), this requires that the interfacial area per surfactant Σ depends on composition as

$$\Sigma \propto \frac{\phi(1-\phi)}{\phi_s \xi_K}, \tag{1.2}$$

where ϕ is the volume fraction of water, $1-\phi$ is the volume fraction of oil, and the volume fraction of surfactant is $\phi_s \ll \phi, 1-\phi$. The JLG model uses a free energy contribution per surfactant

$$F = A(\Sigma - \Sigma_0)^2/\Sigma_0^2. \tag{1.3}$$

This represents the preference of the surfactant layer for an optimum area per molecule Σ_0. The bending energy was estimated by assuming the local radius of curvature of the interfacial film to be everywhere comparable to the lattice size ξ_K. (This improves the original Talmon–Prager formulation in which curvature is concentrated at the edges of the Voronoi polyhedra.)

The JLG model, while appealingly simple, does not predict the experimentally observed three-phase equilibrium (Fig. 1). Instead, there is a two-phase region involving equilibrium between two microemulsions. This is understood as follows: as the surfactant concentration decreases, a uniform phase of the required composition would have $\Sigma \gg \Sigma_0$ [Eq. (1.2)], with a corresponding energy penalty from Eq. (1.3) which can be avoided by phase separation into two phases, each having $\Sigma \approx \Sigma_0$. The line $\Sigma = \Sigma_0$ on the phase diagram, known as the Schulman line[16,17] is everywhere close to the two-phase boundary. For high surfactant concentrations, this model predicts $\Sigma \ll \Sigma_0$, implying a large variation in the area per surfactant; a pure surfactant phase is not allowed, since the surfactant must reside at the oil/water interface.

The next development was the theory of Widom.[18] He introduced a (cubic) lattice of variable side ξ, which he then treated as a variational parameter; the free energy was taken at its minimum over ξ for each composition. In his calculation of the bending energy contributions, Widom essentially followed the formulation of JLG.

Widom departed slightly from JLG in the manner in which the variable interfacial area per surfactant Σ was treated. Specifically, he treated the interfacial layer as an ideal gas of surfactant in two dimensions. In conjunction with a bare interfacial tension γ between oil and water, this gives a quadratic minimum in the free energy as a function of the area per head Σ. This is basically the same as Eq. (1.3); however, the coefficient A in that expression is always of order T. Thus this model describes a highly compressible surfactant film at the oil–water interface. While this may be appropriate under some conditions, there are other cases in which the surfactant layer is more like an incompressible two-dimensional liquid. For example, measurements on globular[2] and bicontinuous[25] microemulsions show that that the interfacial area per polar head remains approximately constant under a wide range of conditions, even in the presence of cosurfactant; moreover, measurements on Langmuir monolayers of similar surfactants[19] show that the Σ found directly from studies of microemulsions[6] indeed corresponds to a relatively incompressible fluid state.

Nonetheless, Widom's model succesfully predicts three-phase equilibrium involving a middle-phase microemulsion. For sensible choices of microscopic energy parameters, the predicted structural length scale ξ for the balanced middle phase is of order 100 Å, in accordance with experiments.[6] This middle phase coexists with two nearly pure phases that have $\xi \approx a$, where a is a molecular cutoff. However, curvature fluctuations and the resulting persistence length of the surfactant film are not addressed by this model. In the limit when both K and γ are large, Ref. 18 predicts that

$$\xi \sim a(K\gamma a^2/T^2)^{1/3} e^{\gamma a^2/3T}. \tag{1.4}$$

This is unrelated to the expression (1.1) for the de Gennes–Taupin persistence length ξ_K. Experiments[1,9] indicate (albeit indirectly) that the properties of the middle phase are very sensitive to the properties of the surfactant, implying a strong dependence on the bending constant K. For example, to make a middle phase at all one usually requires cosurfactants such as alcohol, which are expected to reduce K significantly, while having very little effect on the bare surface tension γ. Similarly, the choice of surfactant itself is found to strongly influence the structural properties of the middle phase.[1,16] In the limit of large K, this choice only enters Eq. (1.4) through a weak power-law dependence on K (the bare interfacial tension γ is, by definition, independent of the choice of surfactant). For small values of K/T, Widom's model does predict a stronger dependence on K of the properties of the middle phase.

C. The present work

Our model and its results have previously been summarized.[26] In formulating our model we follow Refs. 17 and 18 in approximating the oil–water domain structure by a coarse-grained lattice. Similarly, a random mixing approximation is used to calculate both the entropy of mixing of the domains, and the extent of the oil–water interface; all the surfactant is assumed to reside at this interface. We depart from Ref. 17, and follow Ref. 18, in assigning to our lattice a variable cell size ξ; however, rather than being a variational parameter, ξ will be determined uniquely by the volume fractions of oil, water, and surfactant. This is because we treat the surfactant layer at the oil–water interface as an incompressible two-dimensional fluid: $\Sigma \equiv \Sigma_0$ is a fixed constant. The volume fraction of surfactant is then proportional to the total area of the oil–water interface, which is a known function of the water and oil volume fractions, and ξ, once the random mixing approximation is made.

Formally we may consider the fixed Σ constraint to arise as a limiting form of the free energy (1.3), in which the coefficient A obeys $A/T \to \infty$. This limit is complementary to that of Widom's model, in which A/T remains always of order unity. To obtain $A/T \to \infty$ in that model would require: (i) the incorporation of hard-core repulsions between the surfactant molecules at the interface; (ii) taking the limit $\gamma \to \infty$. Once Σ is fixed, the bare oil–water interfacial tension γ, may be absorbed into the chemical potential of the surfactant, and plays no further role in the theory. This is in contrast to the major role played by γ in Widom's model (at least in the limit of $K/T \gg 1$).

The characterization of the microemulsion by the single length scale ξ is implicit in the mean-field approach used here and by other authors.[16–18] The theory does not account for the presence of small amounts of surfactant dissolved in the coherent oil and water domains of the microemulsion. The effects of these components on phase equilibria is somewhat delicate, and could in principle led to the destabilization of the three-phase equilibrium that we find. However, a self-consistent treatment of these effects would involve consideration of polydispersity effects on a multiplicity of length scales, which is beyond the scope of the present work.

Our second major departure from the previous formulations lies in the treatment of the bending energy. Helfrich,[27] and Peliti and Leibler,[28] have shown that the bending constant K of a flexible sheet of size ξ is renormalized downwards by thermal undulations at long length scales. In first-order perturbation theory, these authors found a size-dependent effective bending constant $K(\xi)$ which obeys

$$K(\xi) = K_0[1 - \tau \log(\xi/a)], \tag{1.5}$$

where $K_0 \equiv K(a)$ is the bare bending constant (denoted previously by K); a is a molecular length which provides the cutoff wavelength of undulation modes [cf. Eq.(1.1)]; and

$$\tau = \alpha T/4\pi K_0. \tag{1.6}$$

Here α is a numerical constant, whose precise value ($\alpha = 1$, or $\alpha = 3$) remains in dispute.[27–29] In the remainder of this article, we will choose $\alpha = 1$. It is convenient to choose Eq. (1.6) as a definition of the arbitrary parameter α in Eq. (1.1) for the persistence length ξ_K. In this case, Eq. (1.4) becomes

$$K(\xi) = -\tau K_0 \log(\xi/\xi_K). \tag{1.7}$$

The downward renormalization of K indicates that it becomes relatively easy to bend a sheet of size $\xi \geqslant \xi_K$, since such a sheet is anyway spontaneously crumpled. The perturbative result (1.5) must fail for $\xi \geqslant \xi_K$ since mechanical stability requires $K \geqslant 0$. However, for $\xi \leqslant \xi_K$ the form (1.5) should give the correct qualitative behavior.

In our model for microemulsions (Sec. II), the renormalization of the bending constant is incorporated by identifying the length scale ξ in Eq. (1.5) with the lattice constant used in the coarse graining of the oil and water domains. This captures the fact that there is little to be gained, in terms of bending energy, by having domains much larger than ξ_K, the persistence length of the surfactant film. This is because such a domain has a wrinkled surface, and so may as well break up into smaller pieces (thus gaining entropy of mixing). Of course it was precisely this physical idea that motivated JLG to set $\xi = \xi_K$ in their model; however that turned out to be too restrictive an assumption to give three-phase equilibrium, since when the compositions approach those of pure water or oil (as for the nearly pure phases with which the middle phase coexists) the domains may be much smaller than ξ_K. In our model,[30] we find a middle-phase microemulsion for which the structural length scale ξ is indeed comparable to ξ_K as defined by Eq (1.1); but this is a result of the theory, rather than an initial assumption. We note that the variation of the middle-phase cell size with the persistence length represents an unusual dependence of the phase behavior on thermal fluctuations. These are of importance even in three-dimensional microemulsions because their properties are determined by the nature of the thermal fluctuations of the two-dimensional surfactant film.

The organization of the paper is as follows: In Sec. II we present a phenomenological model which combines features of both the JLG model and that of Widom. Section III describes extensions of our model to account more carefully for the properties of the nearly pure phases that coexist with the middle-phase microemulsion. In that section we also consider the stability of the microemulsion relative to lamellar phases. Section IV contains a further discussion and a summary of our results.

II. THE BASIC MODEL

A. Free energy of a random microemulsion phase

With the assumptions of the previous section, we consider microemulsions to be ternary mixtures of oil, water, and surfactant. Space is divided into cubes of size ξ filled either with water or oil. The surfactant is constrained to stay at the water–oil interface (Fig. 2); we divide it equally between the oil and water domains. Using the random mixing approximation, the probability ϕ for a cube to contain water is

$$\phi = \phi_w + \phi_s/2,$$

where ϕ_w and ϕ_s are, respectively, the volume fractions of water and surfactant. The probability for a cube to contain oil is $1 - \phi$. The constraint for the surfactant to fill the water–oil interface allows us to relate the volume fractions of the components and the lattice size ξ within the random mixing approximation:

$$\phi_s \Sigma_0 = z v_s \frac{\phi(1-\phi)}{\xi}, \tag{2.1}$$

where $z = 6$ is the coordination number of the cubic lattice;

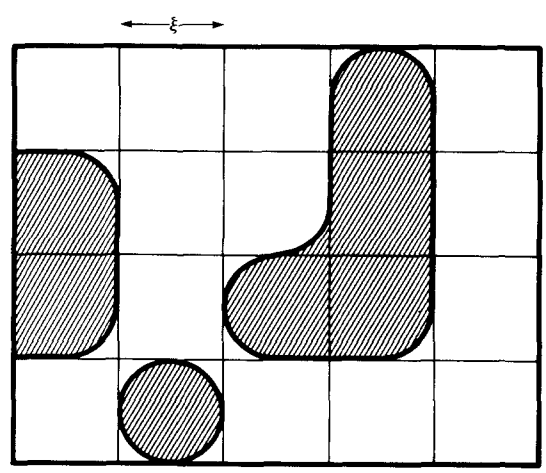

FIG. 2. A typical water, oil, and surfactant configuration in the random-mixing approximation is shown schematically. The shaded region represents the water domains, the thick line delineates the surfactant film, and the remainder of the volume is filled with oil.

v_s is the molecular volume of the surfactant and Σ_0 is the surface area per polar head of a surfactant molecule, which is fixed in our model. Within this approximation the relation (2.1) gives the lattice size ξ at each point of the phase diagram

$$\frac{\xi}{a} = z\frac{\phi(1-\phi)}{\phi_s}, \tag{2.2}$$

where, for convenience, $a = v_s/\Sigma_0$ is chosen to be equal to the lower cutoff in Eqs. (1.1) and (1.5). Note that in our model, the lattice size ξ is neither fixed at a constant value (as in the JLG model) nor a variational parameter (as in Widom's model) but is determined by the constraint, Eq. (2.2).

Since the area per polar head is kept fixed, the free energy per unit volume f has only two terms: the entropy of mixing of the water and oil domains f_s and the energy of curvature of the interface f_c. The first term is calculated using the random mixing approximation

$$f_s = \frac{T}{\xi^3}[\phi\log(\phi) + (1-\phi)\log(1-\phi)] \equiv \frac{T}{\xi^3}S(\phi). \tag{2.3}$$

The second term f_c is calculated as follows. First we associate the bending energy E_c of a cube of water (oil) of size ξ surrounded by oil (water) with that of a sphere of diameter ξ:

$$E_c = 8\pi K(\xi)(1-\xi/\rho_0)^2,$$

where ρ_0 is twice the spontaneous radius of curvature and is defined to be positive for curvature towards the water and negative for curvature towards the oil. In our model the probability of having a bend is related to the probability of having an edge. However, we take the radius of curvature to be comparable to ξ, rather than presuming the interface to have a sharp edge. Thus, the total energy of curvature per unit volume is given by

$$f_c = \frac{8\pi K(\xi)}{\xi^3}[\phi(1-\phi)^2(1-\xi/\rho_0)^2 + \phi^2(1-\phi)(1+\xi/\rho_0)^2] \tag{2.4a}$$

$$= \frac{8\pi K(\xi)}{\xi^3}\phi(1-\phi)[1-2\xi(1-2\phi)/\rho_0] + \cdots. \tag{2.4b}$$

In Eq. (2.4b), we have dropped a term linear in ϕ_s which may be absorbed into the chemical potential of surfactant. The numerical factor in Eq. (2.4) was determined by choosing the bends to be sections of a sphere. This choice is somewhat arbitrary, a fact which limits the sensitivity of our calculation to the exact value of α in Eq. (1.1).

As explained in Sec. I, we have explicitly incorporated in our model the renormalization of the bending constant by thermal fluctuations. The bending constant $K(\xi)$ is then explicitly a function of the lattice size ξ, Eq. (1.5), and is a decreasing function of ξ. The total free energy per unit volume f is the sum of f_s, Eq. (2.3), and f_c, Eq. (2.4b). We can rewrite the free energy in reduced units, defining

$$\tau = \alpha T/(4\pi K_0), \tag{2.5a}$$

$$\delta = \xi_K/a = \exp(1/\tau), \tag{2.5b}$$

$$x = \xi/\xi_K, \tag{2.5c}$$

$$x_0 = \xi_K/\rho_0, \tag{2.5d}$$

$$\tilde{\phi}_s = \phi_s\delta. \tag{2.5e}$$

We also define the reduced free energy $f_r = (\xi_K^3/T)f$,

$$f_r = \frac{1}{x^3}\{S(\phi) - 2\phi(1-\phi)\log(x) \times [1 - 2xx_0(1-2\phi)]\}. \tag{2.6}$$

The factor of 2 which multiplies the entire second term of Eq. (2.6) comes from our association of the bends with sections of a sphere. A different geometrical relationship would change this factor, as would a change in α. The constraint given by Eq. (2.2) becomes

$$x = 6\frac{\phi(1-\phi)}{\tilde{\phi}_s}. \tag{2.7}$$

Equations (2.6) and (2.7) define a reduced free energy $f_r(\phi,\tilde{\phi}_s)$ as a function of the two compositions ϕ and $\tilde{\phi}_s$. This free energy is universal in the sense that, in reduced units, it does not depend on the value of K_0. There is only one parameter: x_0, the reduced spontaneous curvature. All the lengths are in units of ξ_K and the energies in units of T.

B. Main characteristics of the free energy

We first consider the simple case where x_0 is equal to zero (symmetrical case of no spontaneous curvature). The function $f_r(\phi,\tilde{\phi}_s)$ is a function whose properties determine the phase diagram. Figure 3 shows a series of sections through the surface at fixed $\tilde{\phi}_s$ and variable ϕ. For $\tilde{\phi}_s$ greater than a maximum value $\tilde{\phi}_{s_m} = 12/e \approx 4.4$, $f_r(\phi,\tilde{\phi}_s)$ has only one minimum at $\phi = 0.5$. For $\tilde{\phi}_s$ smaller than $\tilde{\phi}_{s_m}$, the function has two minima, and a maximum at $\phi = 0.5$ as shown in Fig. 3. As the value of $\tilde{\phi}_s$ further decreases, these minima approach the limiting values $\phi = 0$ and $\phi = 1$ and the value of the free energy at these minima diverges to $-\infty$. Similar behavior was noticed by Widom[18] and corresponds to the fact that the entropy of mixing favors small values of ξ. In

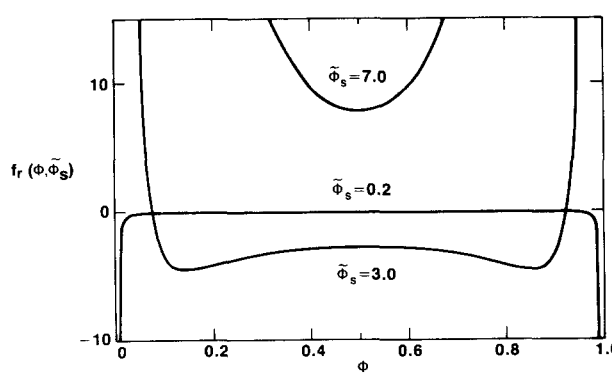

FIG. 3. Sections through the reduced free energy surface, Eq. (2.6), for variable $\phi = \phi_w + \phi_s/2$ and fixed $\tilde{\phi}_s = \phi_s\delta$, where ϕ_w is the water volume fraction, ϕ_s is the surfactant volume fraction, and $\delta = \exp(1/\tau)$ [see Eq. (2.5)]. One minimum at $\phi = 0.5$ is seen for $\tilde{\phi}_s = 7.0$, whereas for $\tilde{\phi}_s = 3.0$ there are two minima. For even lower values of $\tilde{\phi}_s$, $\tilde{\phi}_s = 0.2$, the two minima are very close to the corners at $\phi = 0$ and $\phi = 1$.

order to obtain a more physical result he introduced a cutoff for the lattice size at $\xi = a$, a being a molecular length. In our model, the finite volume of the surfactant will naturally take care of this problem. Indeed, for a given amount of surfactant, ϕ cannot be smaller than $\phi_s/2$ or greater than $1 - \phi_s/2$ (these values correspond to a lattice size $\xi \sim a$). Consequently, in our model the limit of the accessible region for the variables (ϕ and $\tilde{\phi}_s$) is a triangle defined by $\phi \geqslant \tilde{\phi}_s/2\delta$ and $\phi \leqslant 1 - \tilde{\phi}_s/2\delta$. The minima of $f_r(\phi)$ at constant $\tilde{\phi}_s$ reach the boundaries at a critical value of $\tilde{\phi}_s$, $\tilde{\phi}_{s_c} = 18/\delta$: for values of $\tilde{\phi}_s$ smaller than $\tilde{\phi}_{s_c}$ the minima are on the boundaries of the phase diagram (Fig. 3). We summarize this behavior in Fig. 4 where we show the contour plot of the free energy surface. In addition to a saddle point (point S, where $\phi = 0.5$), two deep minima are located very near the corners on the oil–surfactant side and on the water–surfactant side.

The free energy exhibits a region where the curvature of the surface (second derivative) is negative. The instability of the system is an indication of the existence of a phase separation. The phases in equilibrium consist of either two symmetrical microemulsions or three phases. Because the free energy is symmetric in $\phi \leftrightarrow (1 - \phi)$, we find the three-phase equilibrium by plotting the value of the free energy at the minimum ϕ_m, as a function of $\tilde{\phi}_s$. In Fig. 5 the function $f_r[\phi_m(\tilde{\phi}_s), \tilde{\phi}_s]$ is shown schematically. This function is divided in three parts corresponding to the three different regimes previously described. For $\tilde{\phi}_s > \tilde{\phi}_{s_m}$ there exists only one minimum for $\phi = 0.5$. For $\tilde{\phi}_{s_c} < \tilde{\phi}_s < \tilde{\phi}_{s_m}$ there exist two minima where $(\partial f/\partial \phi)_{\tilde{\phi}_s} = 0$. When $\tilde{\phi}_s < \tilde{\phi}_{s_c}$ the two minima are given by the intersection of the free energy with the boundaries of the phase diagram and $(\partial f/\partial \phi)_{\tilde{\phi}_s} \neq 0$. Figure 5 exhibits a region of instability (between the points A, where $\tilde{\phi}_s = \tilde{\phi}_{s_c}$, and B, where $\tilde{\phi}_s > \tilde{\phi}_{s_m}$). At these points a phase separation to three coexisting phases occurs, since the point A corresponds to two symmetrical roots and B to one.

The method explained above is a simplified geometrical version, in the symmetric case, $x_0 = 0$, of the common tangent plane construction. However, the determination of the boundaries of the two-phase regions, or indeed the whole phase diagram for the case of $x_0 \neq 0$, requires a numerical calculation as discussed in the following section.

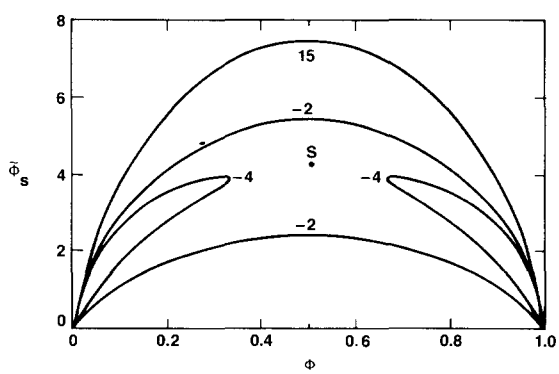

FIG. 4. Contour plot of the reduced free energy, $f_r = -4, -2$, and $+15$, as a function of ϕ and ϕ_s for $x_0 = 0$ and $\tau = 0.2$. The point labeled S is a saddle point. Two deep minima exist close to the oil and water corners at $\phi_s = 0$, $\phi = 0$ and 1, respectively.

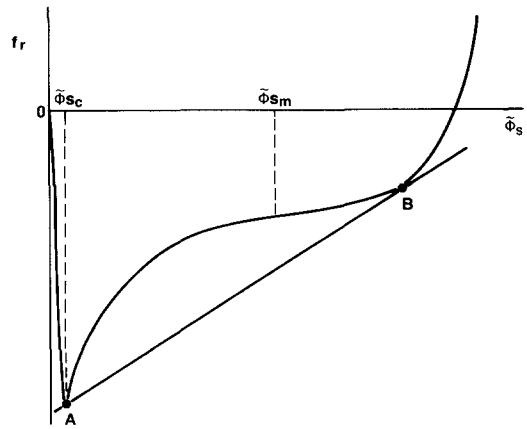

FIG. 5. A schematic plot of the reduced free energy, Eq. (2.6), evaluated at its minimum with respect to ϕ and then plotted as a function of $\tilde{\phi}_s$. A three-phase coexistence is demonstrated here via the common tangent construction. Point A corresponds to the dilute phases (water and oil) and point B is the middle-phase microemulsion. The inflection point at $\tilde{\phi}_s = \tilde{\phi}_{s_m}$ and the deep minima at $\tilde{\phi}_s = \tilde{\phi}_{s_c}$ are shown.

C. Calculation of the phase diagram

To calculate the phase diagram (Fig. 6) we define the potential

$$g(\phi, \tilde{\phi}_s) = f_r(\phi, \tilde{\phi}_s) - \mu_\phi \phi - \mu_s \tilde{\phi}_s. \tag{2.8}$$

The equivalent of the common tangent construction on

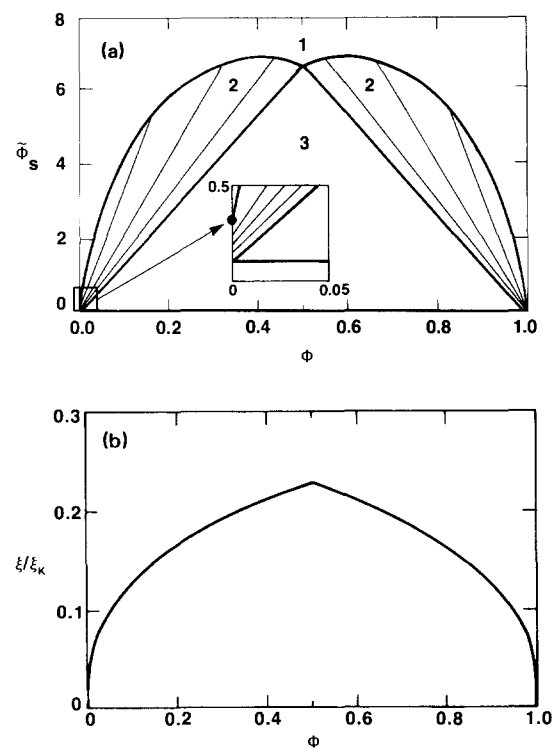

FIG. 6. (a) Phase diagram for the case of no spontaneous curvature ($x_0 = 0$). The numbers denote the number of coexisting phases and the tie-lines in the two-phase regions are shown. The inset shows the details of the tie lines at small values of the volume fractions. The value of $\tau = 0.2$ was used. (b) Variation of ξ/ξ_K (the normalized length scale of the microemulsion defined as x in the text) along the two-phase boundary.

$f_r(\phi,\tilde{\phi}_s)$ is the minimization of $g(\phi,\tilde{\phi}_s)$ with respect to ϕ and $\tilde{\phi}_s$ with fixed values of the chemical potentials μ_ϕ and μ_s. We solve the system of two equations defined by

$$\left(\frac{\partial g}{\partial \phi}\right)_{\tilde{\phi}_s} = 0 \quad \text{and} \quad \left(\frac{\partial g}{\partial \tilde{\phi}_s}\right)_{\phi} = 0, \tag{2.9}$$

the resulting phase diagram is shown in Fig. 6.

The absolute minimum of the function g corresponds to the stable phase at a given chemical potential. In practice Eqs. (2.9) were solved numerically yielding the values ϕ_1 and $\tilde{\phi}_{s_1}$. The resulting solution competes with that corresponding to the free energy minima situated on the boundaries of the phase diagram. Due to the finite volume fraction surfactant, these minima do not correspond to a point where the first derivatives of the free energy are equal to zero. Consequently, we must compare the solution given by Eq. (2.9) with that found by minimizing the function g along the boundaries of the phase diagram

$$\frac{dg(\tilde{\phi}_s/2\delta,\tilde{\phi}_s)}{d\tilde{\phi}_s} = 0 \tag{2.10}$$

for the water–surfactant side and

$$\frac{dg(1-\tilde{\phi}_s/2\delta,\tilde{\phi}_s)}{d\tilde{\phi}_s} = 0 \tag{2.11}$$

for the oil–surfactant side.

Equations (2.10) and (2.11) give two other sets of solutions situated on the limit of the phase diagram ($\phi_2 = \tilde{\phi}_{s_2}/2\delta, \tilde{\phi}_{s_2}$) and ($\phi_3 = 1 - \tilde{\phi}_{s_3}/2\delta, \tilde{\phi}_{s_3}$). The values of the free energy g at the three minima $g_i = g(\phi_i,\tilde{\phi}_{s_i})$, $i = 1,2,3$, allow us to determine the phase diagram. The values of μ_ϕ and μ_s, where two or more minima are equal, determine the chemical potentials for which two or more phases coexist. The solution $(\phi_i,\tilde{\phi}_{s_i})$ gives the location of the phases in equilibrium. In Sec. III we will, in addition, compare the free energy of the microemulsion with the free energy of a lamellar phase using the same procedure.

The preceding calculation leads to the phase diagram shown in Fig. 6(a). It exhibits a one-phase region (the microemulsion phase) and three polyphasic regions: two two-phase regions where a microemulsion phase is in equilibrium with a very dilute phase of surfactant in water or oil (upper- or lower-phase microemulsions, respectively), and a three-phase region where a middle-phase microemulsion is in equilibrium with both dilute phases.

Figure 6(b) is a plot of the reduced length scale, $x = \xi/\xi_K$ along the two-phase coexistence curve. We have chosen $\tau = 0.2$, which corresponds to $K_0/T \sim 0.4$ for $\alpha = 1$. (Measured values of $K_0/T < 1$ have been reported in Ref. 31.) For this choice of τ, $\xi \approx 0.23\xi_K$. Moreover, ξ remains on the order of ξ_K even far from the middle phase. It is only when ϕ is very close to 0 or 1 that ξ falls rapidly to a microscopic value ($\xi \sim a$).[30] In addition, the concentration of surfactant in the middle phase[32] scales as $\log \phi_s \sim -1/\tau \sim -K_0/T$. Thus the volume fraction of surfactant can be very small, when ξ_K is large compared to the molecular length. Consequently, the phase diagram is a strong function of ξ_K (and therefore of K_0/T) when plotted as a function of the unscaled volume fractions. However, the phase diagram as a function of the scaled volume fraction $\tilde{\phi}_s$ is practically independent of the value of ξ_K. The cusp that occurs at $\phi = 0.5$ [Fig. 6(b)], has its origin in the crossover of the two-phase equilibrium from that of a microemulsion with water to a microemulsion with oil.

The detailed structure in the corners of the phase diagram is given in the inset of Fig. 6(a). All the tielines of the two-phase equilibria start from the boundaries of the phase diagram (water–surfactant and oil–surfactant sides). The points where the coexistence curves reach the limits of the phase diagram are critical points. Indeed at these points the composition of the two phases in equilibrium becomes identical.[33] It should be noted, however, that we do not expect our free energy to be accurate in this region of the phase diagram. We will see in the next section that we can generalize our model to include a more realistic account of the properties of the dilute phases.

We now consider the case of finite spontaneous curvature ($x_0 \neq 0$). We choose $x_0 > 0$; the case $x_0 < 0$ corresponds to the same evolution of the phase diagram but with the oil and water volume fractions interchanged. So long as the spontaneous radius of curvature remains larger than or on the order of ξ_K ($x_0 < 1$) the phase diagram shows a slight asymmetry but the three-phase equilibrium still exists (see Sec. III). However, when the spontaneous curvature x_0 is much greater than 1 ($\rho_0 \ll \xi_K$), the three-phase region vanishes (Fig. 7). The phase diagram is then very asymmetric and most of the two-phase region consists of equilibria between a microemulsion phase and nearly pure water. In this case, along the phase boundary, ξ scales with ρ_0, indicating that phase separation occurs when the typical domain size is of the order of ρ_0. This result is an indication of the emulsification failure[3] instability that precludes the formation of globules with a size larger than ρ_0. It is also interesting to notice that the three-phase equilibrium disappears when $x_0 = \xi_K/\rho_0$ is of order unity.

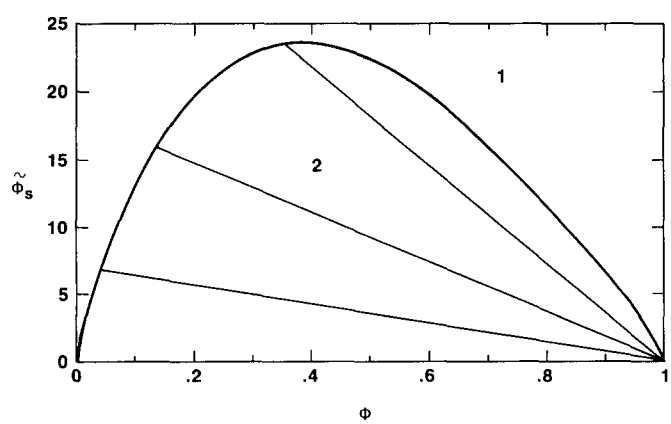

FIG. 7. Phase diagram for finite spontaneous curvature, with $x_0 = \xi_K/\rho_0 = 10$ and $\tau = 0.15$. The tielines in the two-phase region indicate the coexistence of a microemulsion phase with nearly pure water. Both the two-phase coexistence with oil and the three-phase region no longer exist for this value of x_0.

III. EXTENSIONS OF THE BASIC MODEL

A. Generalized phase diagrams

The previous section described the phase diagram obtained from a double-tangent plane construction using the free energy of Eq. (2.6). We now describe a simplified method for generating the two- and three-phase coexistence regions. This method relies on the observation that the microemulsion phases coexist with very dilute phases of surfactant in water or in oil.

Our study of the free energy surface in Figs. 3–5 showed that the three-phase equilibrium is due to the presence of two deep minima in the model free energy, in the region of very small surfactant concentration. However, our model, which describes the surfactant as an almost flat monolayer at the water/oil interface, may not be appropriate in the dilute regime where these minima occur. The extrapolation of the bending energy to dilute phases where the surfactant exists in the form of micelles or isolated molecules in solution may not be justified.

We therefore introduce a simple model for these dilute phases which is, in general, not merely an extrapolation of the microemulsion free energy. Denoting the free energy per unit volume of the dilute phases in water and oil respectively by $\bar{f}_w$ and $\bar{f}_0$, we write[34]

$$\bar{f}_w = T\,[\bar{\phi}_s(\log\bar{\phi}_s - 1) + \chi_w\bar{\phi}_s]/R^3, \tag{3.1}$$

where $\bar{\phi}_s$ is the volume fracion of surfactant in the dilute phase and R^3 is the volume of a micelle. The first term in Eq. (3.1) is the entropy of mixing and the second term is the energy of surfactant in dilute solution. Note that the zero of energy is that of a flat surfactant monolayer. Thus, if the surfactant free energy is lowest for saturated interfaces, the dimensionless energy χ_w of the micelle or isolated surfactant in solution is positive.[35] It is only the entropy of mixing that stabilizes these dilute phases with respect to the microemulsion phases. A similar expression is used for the free energy per unit volume of the oil-rich dilute phases with $\bar{f}_w \to \bar{f}_0$ and $\chi_w \to \chi_0$.

Note that the dilute limit of our microemulsion free energy, Eq. (2.6) with $x_0 = 0$, reduces to the form of Eq. (3.1), with $R = 6^{1/3}a$ and $\chi_w = 8\pi K_0/T$, for $\chi_w \gg 1$. The recognition that the dilute phases cannot necessarily be described by the same harmonic bending energy as the microemulsion phases is expressed by the introduction of a new energy χ_w, which is not simply related to K_0. Note that one could also have introduced this connection by considering higher order terms in the bending energy. These would scale as

$$K^* a \int \left(\frac{1}{R_1} + \frac{1}{R_2} - \frac{2}{\rho_0}\right)^3 dS. \tag{3.2}$$

Since the surface area is proportional to terms quadratic in R_1 and R_2, these higher order terms are negligible for large values of R_1 or R_2 (i.e., in microemulsions). They become important only in the states where both R_1 and R_2 are comparable to the molecular size a (i.e., in the micellar or surfactant solutions). The anharmonic coefficient K^* would then be related to χ_w or χ_0 of Eq. (3.1). One would then have a single expression for the free energy which would describe the different energetics of both the microemulsion and dilute phases. In the following, however, we use Eq. (3.1) for the modeling of the dilute phases treating χ_w and χ_0 as phenomenological parameters.

Recalling the coexistence curves of Fig. 6, we now look for an equilibrium of a three-component (water–oil–surfactant) microemulsion with a two-component (water–surfactant or oil–surfactant), dilute phase. The equations for two-phase equilibrium of the microemulsion with a dilute phase of surfactant in water are

$$f + (1-\phi)\frac{\partial f}{\partial\phi} - \phi_s\frac{\partial f}{\partial\phi_s} = \bar{f}_w - \bar{\phi}_s\frac{d\bar{f}_w}{d\bar{\phi}_s}, \tag{3.3}$$

$$\frac{\partial f}{\partial\phi_s} - \frac{1}{2}\frac{\partial f}{\partial\phi} = \frac{d\bar{f}_w}{d\bar{\phi}_s}. \tag{3.4}$$

Equation (3.4) results from the equality of the chemical potential for surfactant which exists in both the microemulsion and dilute phases. The second term in Eq. (3.4) arises from the dependence of ϕ in the microemulsion phase on ϕ_s. For a dilute phase of surfactant in water, Eqs. (3.1) and (3.4) determine the value $\bar{\phi}_s = \phi_s^*$ as

$$\log\phi_s^* = -\chi_w + \left[\frac{\partial f}{\partial\phi_s} - \frac{1}{2}\frac{\partial f}{\partial\phi}\right]R^3/T. \tag{3.5}$$

Since f in the microemulsion phase is of order T/ξ_K^3, where $\xi_K/a \sim \exp(1/\tau) \gg 1$, and since $\phi_s \sim a/\xi_K$ in the middle phase, the second term is of the order of $(a/\xi_K)^2$. Thus, for large values of ξ_K, the first term on the right-hand side of Eq. (3.5) dominates. Equation (3.5) shows that the value of ϕ_s^* in the dilute phases is approximately independent of the value of ϕ or ϕ_s in the coexisting microemulsion phases.

Similar considerations allow us to neglect the second term on the right-hand side of Eq. (3.3). With these approximations, the above equations reduce to only one condition:

$$f + (1-\phi)\frac{\partial f}{\partial\phi} - \phi_s\frac{\partial f}{\partial\phi_s} = f_w^*, \tag{3.6}$$

where now $f_w^* = \bar{f}_w(\phi_s^*)$, with $\phi_s^* \approx \exp(-\chi_w)$. The phase boundary for two-phase coexistence is then found directly by plotting ϕ_s as a function of ϕ as given by Eq. (3.6). If the value $\chi_w = 8\pi K_0/T$ is used, the results are indistinguishable from those of the exact tangent plane construction (see Fig. 6) described in Sec. II, except for a region very close to the corners of the phase diagram [seen only in the inset of Fig. 6(b)]. Our approximation is equivalent to having the ends of the tielines in Fig. 6 meet at a single point. In addition, by choosing different values of χ_w and χ_0, we can generalize the results of Sec. II. [Note that Eq. (3.1) can be generalized to even more accurately model the free energy of the dilute phases.] For example, the inclusion of attractive interactions may further destabilize the micellar phase.

We have just described a simplified generalization for determining the coexistence of a microemulsion with dilute phases of surfactant in water or oil. The independent modeling of the free energy of dilute surfactant solutions introduces two new relevant energy scales χ_w and χ_0, in addition to K_0. Since $f_w^* \sim T\exp(-\chi_w)/a^3$, we can equally well parametrize the dilute phases by f_w^* or f_0^*. The coexistence curves are in general sensitive to the values of these parameters. For example, Fig. 8 shows that if $f_w^* \neq f_0^*$, the phase

diagram is not symmetric about $\phi = 0.5$, even though the microemulsion phase has no preferred curvature ($x_0 = 0$). This is because phase equilibria are sensitive to the global properties of the free energy surface, including the behavior close to the corners of the three-phase triangle. Although there is no spontaneous bending of a surfactant film towards either water or oil, the different free energies of isolated surfactant molecules or micelles in water-rich and oil-rich environments can be different. If f_w^*/f_0^* is very different from unity, the three-phase region can entirely disappear. There are thus two mechanisms which can give rise to an asymmetry of the phase diagram, and in the extreme case, to the disappearance of the three-phase equilibrium: (i) a finite spontaneous curvature, $x_0 \neq 0$; (ii) a difference in the free energies of the surfactant in the dilute phases, $f_w^* \neq f_0^*$.

B. Two-phase coexistence

In the previous section, we showed that the phase diagram can be obtained quite simply by looking for coexistence of a microemulsion with a dilute surfactant solution, characterized by a free energy f^*, which is in general, distinct from the dilute limit of the microemulsion free energy f. [Here we assume $f_w^* = f_0^* = f^*$.] This approximation relies on the occurence of a deep minimum in f as a function of the surfactant volume fraction ϕ_s. As previously stated, if f^* becomes comparable to the free energy of the middle phase f, two two-phase equilibria of microemulsion and water-rich or oil-rich dilute surfactant phases and the associated three-phase region, disappear. In their stead, a two-phase equilibrium between two microemulsion phases arises.

We restrict the discussion to the case of no spontaneous curvature for which the two coexisting microemulsion phases with the same values of ϕ_s are found from the equality of the water or oil chemical potentials. Since f is invariant to a change of ϕ to $(1-\phi)$, the oil and water chemical potentials have opposite sign. The equality of the two chemical potentials then implies

$$\left(\frac{\partial f}{\partial \phi}\right)_{\phi_s} = 0. \tag{3.7}$$

For large negative values of f^*, the coexistence curve determined by Eq. (3.7) lies within the multiphase regions and is thus not observable (see Fig. 9). As f^* increases, the phase diagram goes through the sequence shown in Fig. 9. We see that a criterion for a stable middle-phase microemulsion is that the surfactant not be too insoluble in the dilute phases.[36] Examination of the phase diagrams shows that $f^* < -5T/\xi_K^3$ for the middle-phase microemulsion to exist rather than equilibrium between two microemulsion phases.

When the critical point of two-phase equilibrium at $\phi = 0.5$ occurs at a value of ϕ_s which is approximately equal to the value of ϕ_s for the middle-phase microemulsion, the microemulsion phase itself may be characterized by large concentration fluctuations. This would invalidate the random-mixing approximation used here. The corrections to our model due to correlations between oil and water regions are outside the scope of this work.

C. The lamellar phase

In this section, we consider the relative stability of random microemulsions compared with a lamellar phase which consists of an ordered array of surfactant monolayers dividing adjacent oil and water domains. For the case of no spontaneous curvature, we show that for values of K_0/T that do not exceed a critical value, the random microemulsion is more stable than the lamellar phase at small values of ϕ_s. The renormalization of the bending constant to values of the order of T, allows the energy cost of the random system to be compensated by the entropy gain from the random mixing of water and oil regions. At large values of ϕ_s, the bending constant approaches its bare value K_0. The energy cost of the curved interfaces in the random microemulsion is no longer compensated by the entropy of mixing, and the lamellar phase dominates.

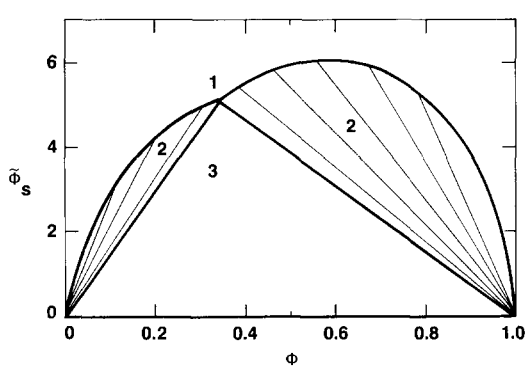

FIG. 8. Phase diagram for no spontaneous curvature ($x_0 = \xi_K/\rho_0 = 0$) and $\tau = 0.2$ for the case of asymmetry in the free energies of the dilute phases ($f_w^* \neq f_0^*$). Here, $f_w^* = -15T/\xi_K^3$ and $f_0^* = -15T/2\xi_K^3$.

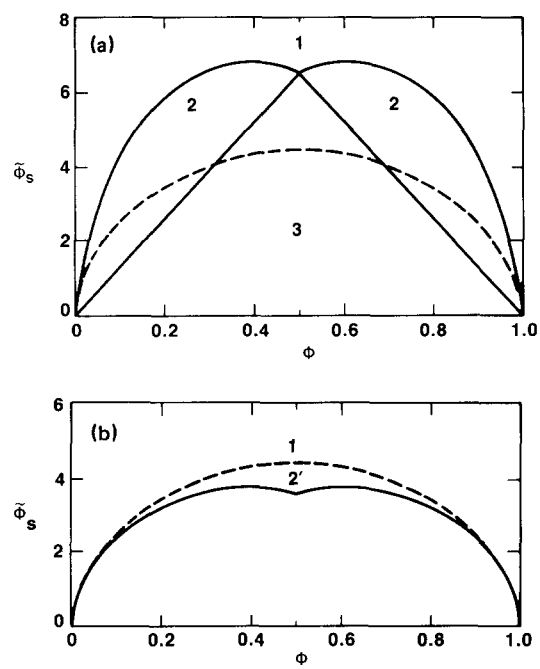

FIG. 9. Phase diagrams including the coexistence of the two microemulsion phases with the same values of ϕ_s (denoted by 2′ and shown by dashed lines). The solid lines represent the multiphase regions of the microemulsion [see Fig. 6(a)]. In (a) the phase diagram is for $f_w^* = f_0^* = -50T/\xi_K^3$, while in (b) $f_w^* = f_0^* = 0$. Note that in (b), the equilibrium is between two microemulsions. The value of $\tau = 0.2$.

We compare the free energies of the microemulsion and lamellar phases. Although the ordered, lamellar phase has no entropy of mixing and no curvature energy, it has a finite free energy due to the steric repulsion of the surfactant sheets.[37,38] This repulsion reduces the meandering entropy of the lamellae from its value in the limit of infinite separation of the surfactant sheets.[39] The additional free energy per unit volume has been estimated by Helfrich[37] for an ordered array of lamellae in a single solvent and is proportional to the product of the number of lamellae per unit length and $T^2/(K_0 d^2)$. In our case, the lamellae separate adjacent regions of oil and water. We heuristically generalize Helfrich's result to describe the free energy of the lamellar microemulsion per unit volume f_l, and write

$$f_l = \chi T\left(\frac{T}{K_0}\right)\left[\frac{1}{d_0^2}+\frac{1}{d_w^2}\right]\left(\frac{2}{d_w+d_0}\right). \tag{3.8}$$

In Eq. (3.8), $d_0 \approx 2a\phi_0/\phi_s$ and $d_w \approx 2a\phi_w/\phi_s$ are the distances between the surfactant sheets separating oil and water domains, respectively. The surfactant volume fraction is given by $\phi_s = 2a/(d_0 + d_w)$. We expect Eq. (3.8) to be correct for $d < \xi_K$. The parameter χ expresses the uncertainty in the numerical coefficient of Eq. (3.8) which depends on the details of the short distance cutoff. In our numerical calculations, we arbitrarily take $\chi = 0.15/\pi \approx 0.05$; if χ is taken to be Helfrich's value of $(3\pi^2/256) \approx 0.12$, the microemulsion is stable with respect to the lamellar phase even at high values of ϕ_s, for the chosen $\tau = 0.2$.

A determination of the phase diagram is obtained from a double tangent construction on both f_l and f as described in Sec. II above. The results are shown in Fig. 10, for a value of $\tau = T/4\pi K_0 = 0.2$. Since the lamellar free energy scales as $(T^2/K_0)\,\phi_s^3/a^3$, and the microemulsion free energy scales as $T\phi_s^3/a^3$, the free energy difference between them is decreased as K_0 is increased. For large values of K_0/T, the lamellar phase coexists directly with the dilute phases and the middle phase microemulsion disappears. This confirms the suggestion of de Gennes and Taupin,[16] that the lamellar structure is more stable than the random microemulsion for stiff surfactant sheets.

This comparison of the free energies of the lamellar and microemulsion phases, reveals the crucial role that the renormalization of the bending constant plays in our model. It is through this renormalization that the bending energy in the random microemulsion phase is reduced so that the entropy gain of the random structure stabilizes it against the ordered, lamellar phase.[30] In our model, the bending constant is naturally reduced to values of order T by the thermal fluctuations. However, before more definite conclusions can be reached, a more accurate description of the lamellar phase free energy may be needed. Our treatment is a first approximation, and contains the phenomenological parameter χ.

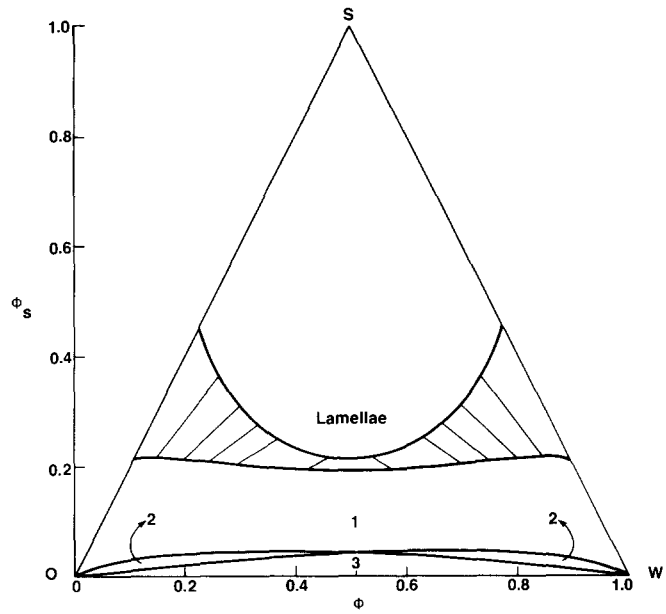

FIG. 10. Phase diagram for microemulsions with no spontaneous curvature ($x_0 = 0$). The region where the lamellar phase is stable is indicated. The numbers indicate the number of coexisting phases. A value of $\tau = 0.2$ was chosen. The tielines indicate the coexistence of disordered microemulsion phases with lamellar phases. The lower part of this phase diagram is the same as in Fig. 6(a), but with a different vertical scale since $\tilde{\phi}_s = \phi_s \exp(1/\tau)$. The phase diagram is drawn within the triangle of allowed concentrations: $\phi_s/2 < \phi$ and $\phi_s/2 < 1 - \phi$.

IV. DISCUSSION

A. Role of microscopic parameters

In the calculations presented here, the microemulsion is assumed to be a ternary mixture of oil, water, and surfactant. Nevertheless, some of the important physical properties and expected phase behavior are obtained. The effects of salinity and cosurfactant (short-chain alcohol) were not taken explicitly into account. Implicitly they enter our model through parameters such as the spontaneous curvature x_0, the bending (rigidity) constant K_0 and the free energies of the dilute phases, f_w^* and f_0^* which were introduced in Sec. III. A more microscopic approach is needed in order to get a quantitative understanding of these parameters and this certainly deserves further investigation. Such an approach might for example give predictions about specific surfactants or surfactant/cosurfactant mixtures.

In studying microemulsions, one should distinguish between ordered phases and disordered, liquid-like ones. For the former, a periodic structure repeats itself on large length scale and the system is generally less like a liquid (viscous, and birefringent in some cases) and more like a weak solid. These phases usually occur at higher surfactant concentration and can range from lamellar to cylindrical or cubic (or others). We discussed in Sec. III a simplified version of such a phase (lamellar). In our view, recent lattice models[21,22] that were proposed for microemulsions are probably more suited to these ordered phases than for the liquid-like disordered ones.

The phases which are the focus of this article as well as previous work,[16–18] are the disordered, liquid-like microemulsion that are useful in many technological applications. Microemulsions, which occur at relatively low surfactant concentration, usually require the addition of salt and cosurfactant for stability. Without these extra components, the phase diagram is usually dominated by lamellar or other ordered phases. The main effects of the salt and cosurfactant are:

(i) To "balance" the hydrophilic–lipophilic interactions, thus effectively reducing the tendency of the surfactant to form globules (driving the spontaneous curvature x_0 towards zero).

(ii) To reduce the rigidity of the surfactant film, thus stabilizing a random configuration of the surfactant interface over a more rigid lamellar structure.

Using a phenomenological lattice model, we presented in Sec. II a simple free energy that predicts the observed three-phase coexistence for a suitable range of our parameters. Our main deviation from previous models is to take into account the renormalization of the bending energy for length scales up to the persistence length. Since we made the simplification that the area per surfactant is fixed, the total area is uniquely determined by the amount of surfactant and we are left only with two terms in our free energy: the entropy of mixing and the bending energy (with a renormalized bending constant which is length-scale dependent).

Cosurfactant does not enter directly into our model but presumably its effect is to reduce the rigidity constant. Both the middle phase and the structural length scale depend very strongly on K_0. Another effect of increasing K_0 is to stabilize lamellar phases when compared to the microemulsion. A moderate value of the bare K_0 (flexible surfactant films) means that the system will have K_0 renormalized to a value of order T at reasonable (~ 100 Å) length scales.

Finally, we note that since the phenomenological parameters (x_0, f_w^*, f_0^*) may in principle be temperature dependent, the phase diagrams can change as the temperature is varied. Hence a useful extension of our model might be to calculate the phase diagram incorporating the temperature dependence of the model parameters. Experimentally, it is found that increasing the temperature can cause either asymmetry towards the oil (e.g., for ethoxylate surfactants[40]) and towards the water (e.g., for sulfonates[10]). In addition, both temperature and K_0 play an important role in the competition between the bicontinuous and lamellar phases as discussed above.

B. Summary of our predictions

We now make a few remarks about our resulting phase diagrams and compare them with previous models:

(i) In the symmetric case ($x_0 = 0$) the calculated phase diagram, Fig. 6, has four distinct regions: a single phase, two two-phase coexistence regions (one consisting of a microemulsion in equilibrium with nearly pure water and the other of a microemulsion in equilibrium with nearly pure oil), and a three-phase region where the middle-phase microemulsion coexists simultaneously with water and oil. The surfactant concentration in the middle phase depends exponentially on the bending constant K_0.

(ii) Deviations from this symmetric picture are observed as we change x_0 from zero to a finite positive (negative) value which reflects a tendency of the surfactant to bends towards the water (the oil). As one increases x_0 from zero, the middle phase moves towards the oil corner. Consequently, the extent of the two-phase coexistence with the water increases while the extent of the two-phase coexistence with the oil decreases until it, as well as the three-phase region, completely disappears (Fig. 7), leaving only the two-phase coexistence between the microemulsion (globules of water in oil) and an excess water phase. This happens at values of $\rho_0 \leqslant \xi_K$ and is in agreement with the concept of an "emulsification failure" instability that was previously discussed for globular microemulsions.[3] The reverse occurs as x_0 is decreased from zero.

With the simple expression that we have for the free energy, Eq. (2.6), x_0 (or ρ_0) is the only parameter that affects the asymmetry of the phase diagram. In Sec. III, we generalized our model and introduced two additional parameters, f_w^* and f_0^*, which are the values of the free energy in the dilute water and oil phases, and are related to the surfactant stability in those phases. In the generalized model, another way to asymmetrize the phase diagram is to increase $|f_w^* - f_0^*|$ while keeping both f_w^* and f_0^* below the microemulsion value. For example, increasing the value of f_0^* with respect to f_w^* causes a shrinking (Fig. 8) of the two-phase coexistence with oil until this coexistence region, as well as that of the three-phase coexistence, disappears.

(iii) Our theory contains several phenomenological parameters such as x_0, f_w^*, and f_0^*, which are related to the surfactant structure and chemistry. These parameters can asymmetrize the phase diagram; they are experimentally controlled through changes in the hydrophilic–lipophilic ratio which depend on temperature (which has other effects as well), salinity, and the stability of water and oil.[41] Since salinity screens the electrostatic interaction in the water, it can be thought of as decreasing x_0 in our model. Also our simplified account of the stability of the dilute water and oil phases in terms of the two parameters f_w^*, and f_0^*, shows that as the stability of the dilute oil phase increases, the oil–microemulsion coexistence region shrinks, until only a coexistence with water is left (no three-phase region). The reverse behavior is seen when the stability of the dilute water phase is increased.

(iv) Another change in the phase diagram occurs as one increases the value of $f^* = f_w^* = f_0^*$ with respect to the microemulsion free energy (Fig. 9). For f^* near zero, the system prefers to separate into two microemulsions, one being oil-rich and the other water-rich (with equal amount of surfactant for the symmetric case $x_0 = 0$). Consequently, the entire three-phase region disappears. This again shows the importance of f^* to the existence of the three-phase region. A similar two-phase coexistence between two microemulsions was also obtained in Refs. 16 and 17. In the JLG model, it was not possible to obtain the three-phase region because the cell size was always presumed to be equal to ξ_K, the persistence length, whereas in our model the cell size varies from $\xi \sim \xi_K$ near the middle-phase point on the phase diagram, to a molecular size for the dilute phases. Similarly, we find coexistence between two microemulsions with unequal amounts of surfactant (oblique tie lines) by introducing a finite spontaneous curvature.

(v) Although our model,[26] Widom's,[18] and Talmon and Prager's[4] all result in three-phase coexistence, there are several important differences between them. In Widom's model the surfactant film is thought of as highly compressible two-dimensional gas whereas in our model it is an in-

compressible film. The stability of the undulating interface in our case is a direct consequence of the renormalization of the bending constant and we find that the structural length scale (cell size) ξ is closely related to the de Gennes–Taupin persistence length ξ_K. It is especially notable (from Sec. III C) that the *smallest* structural length scale ξ obtainable in the microemulsion before phase separation to lamellae occurs, obeys for small τ, $\xi \propto \xi_K \propto e^{1/\tau}$. However, ξ/ξ_K in the middle phase is also bounded above by a constant corresponding to the value obtained at the inflection point $\phi_s = \phi_{s_m}$ as defined in Sec. II B. Thus, the structural length scale ξ in a stable middle-phase microemulsion is always of order ξ_K. Moreover, along the two-phase coexistence lines, ξ deviates strongly from ξ_K only very close to the corners of the phase diagram. This relation between the cell size and the persistence length constant is not found by Widom. For rigid surfactant films, ($K_0 \gg T$) ξ depends only weakly on the bending constant, Eq. (1.4), and exponentially on the water/oil bare surface tension, in his model. This difference between the two theories can be checked experimentally since (within the random mixing approximation) ξ is inversely proportional to ϕ_s the volume fraction of the surfactant. Measurements of K_0 vs ϕ_s and/or ξ in the middle phase will be helpful in comparing these two predictions. In the Talmon–Prager model the phase diagram depends on a parameter (β) in such a way that the middle phase coexists with a phase of 15% oil in water and another of 15% water in oil. In contrast, our middle phase coesists with almost pure water and oil. Another difference is that in our model, the length scale of the domains has a clear physical origin; in the Talmon–Prager model, this length entered as an additional parameter.

(vi) The microemulsion phase should always be compared in stability to more ordered structures such as lamellae (Fig. 10). This was done in Sec. III with some simplifying assumptions about the contribution of thermal fluctuations to the free energy of the lamellar phase. We find that for K_0/T larger than a critical value, the lamellar phase is always more stable than the microemulsion phase and the three-phase coexistence disappears altogether. In contrast, for K_0/T smaller than the critical value, the microemulsion phase is more stable than the lamellar phase for small ϕ_s; as ϕ_s increases, there is a transition (always first order in our model because we are comparing two different branches of the free energy) from an isotropic disordered (microemulsion) phase at small values of ϕ_s to a lamellar one at higher values of ϕ_s. In the coexistence region, the two phases in equilibrium have different values of ϕ and ϕ_s, resulting in the oblique tielines in Fig. 10.

C. Conclusions and future prospects

In this paper, we focused on understanding the origin of middle-phase microemulsions. Within a simple model we calculated phase diagrams that are similar to those observed for nonionic surfactant microemulsions. In addition, our model has a simple physical explanation in terms of the statistical mechanics of the undulating surfactant films separating oil and water regions. The renormalization of the bending constant of such films appears to be crucial to the stabilization of these phases. Indeed, including the effect of the short-wavelength fluctuations is twofold: First, the minimum amount of surfactant ϕ_{s_m} needed to obtain a stable middle-phase scales as the inverse of the persistence length, ξ_K and is an exponential function of the bending constant. Second, it stabilizes the microemulsion phase in comparison with the lamellar phase.[30] Various trends in asymmetrizing the phase diagram were also explored.

A few points deserve additional study; we briefly discuss some of them.

(i) Our calculation as well as those of Refs. 4, 17, and 18 are done within the random mixing approximation, which does not take correctly into account concentration fluctuations. For small length scales (smaller than a cell size), we did include the effects of fluctuations via the renormalization of the bending constant. However, one would like to find corrections to the mean-field approximation for large length scales by writing down a lattice model where the entropy and the bending energy are better approximated.

In addition, the expression used for $K(\xi)$ was derived[27,28] to first order in perturbation theory for zero surface-tension interfaces. This expression is not expected to hold for large length scales. Even within first-order pertubation theory, there is a dispute[27–29] at the present time about the exact value of coefficient α in the expression for $K(\xi)$, Eq. (1.6). Changing α has a similar effect on our phase diagram as changing f^*. Variations in either parameter can cause a crossover from three-phase equilibrium to coexistence between two different microemulsions.

(ii) In our model, Σ, the area per surfactant, is fixed and the bare water/oil surface tension does not enter directly into the free energy. This limit of an incompressible surfactant film is complementary to that of Refs. 17 and 18 where fluctuations around the Schulman line $\Sigma = \Sigma_0$ are allowed. It is possible to generalize our model by taking a variable area per molecule and expanding the free energy around Σ_0. This will introduce a third independent variable (e.g., either Σ, or the cell size ξ) in addition to the two volume fractions ϕ and ϕ_s and requires a minimization with respect to this new variable as well as double tangent construction for the phase diagram. However, if the coefficient A in Eq. (1.3) is large compared with T, the results are qualitatively the same as those of our model, since the departures from the Schulman line are negligible.

(iii) The ultralow interfacial tension σ between microemulsions, and nearly pure water or oil, can be simply understood[16] by the large coherence length in the middle phase, $\xi_K > 100$ Å. From dimensional analysis, one expects that $\sigma \sim T/\xi^2$. Approximating $\xi \sim 50a$, (a being a molecular length), this can explain a reduction of $\sim 10^4$ in the interfacial tension.[13] An additional contribution to the lowering of the interfacial tension may also come from the proximity of the middle phase to a critical point[16,17] where the correlation length of the concentration fluctuations can become very large. We found such a critical point, which, however, will not be observable when it lies within the three-phase region of the phase diagram.

(iv) The comparison of our phenomenological free energy, Eq. (2.6), and the one for the lamellar phase gives a

first-order transition between the two phases when K_0/T is not larger than a critical value. Otherwise the lamellar phase will be more stable than the microemulsion for the entire range of ϕ_s. A more accurate calculation of the free energy of the lamellar phase would enable us to resolve more convincingly the relative stability of random microemulsions and ordered lamellar structures, and possibly other ordered structures such as cubic and cylindrical phases.

ACKNOWLEDGMENTS

The authors acknowledge useful discussions with P. G. de Gennes, R. Goldstein, J. Huang, M. W. Kim, D. Langevin, S. Leibler, R. Reed, C. Safinya, and B. Widom.

[1]For a general survey see (a) *Surfactants in Solution*, edited by K. Mittal and B. Lindman (Plenum, New York, 1984, 1987); (b) *Physics of Complex and Supermolecular Fluids*, edited by S. A. Safran and N. A. Clark (Wiley, New York, 1987).

[2]A. Calje, W. G. M. Agerof, and A. Vrij, in *Micellization, Solubilization, and Microemulsions*, edited by K. Mittal (Plenum, New York, 1977), p. 779; R. Ober and C. Taupin, J. Phys. Chem. **84**, 2418 (1980); A. M. Cazabat and D. Langevin, J. Chem. Phys. **74**, 3148 (1981); D. Roux, A. M. Bellocq, P. Bothorel in Ref. 1(a), p. 1843; J. S. Huang, S. A. Safran, M. W. Kim, G. S. Grest, M. Kotlarchyk, and N. Quirke, Phys. Rev. Lett. **53**, 592 (1983); M. Kotlarchyk, S. H. Chen, J. S. Huang, and M. W. Kim, Phys. Rev. A **29**, 2054 (1984).

[3]C. Huh, J. Colloid Interface Sci. **97**, 201 (1984); **71** (1979); S. A. Safran and L. A. Turkevich, Phys. Rev. Lett. **50**, 1930 (1983); S. A. Safran, L. A. Turkevich, and P. A. Pincus, J. Phys. (Paris) Lett. **45**, L69 (1984).

[4]Y. Talmon and S. Prager, J. Chem. Phys. **69**, 2984 (1978); **76**, 1535 (1982).

[5]L. E. Scriven, in *Micellization, Solubilization, and Microemulsions*, edited by K. Mittal (Plenum, New York, 1977), p. 877.

[6]L. Auvray, J. P. Cotton, R. Ober, and C. Taupin, J. Phys. (Paris) **45**, 913 (1984), and in Ref. 1.

[7]E. W. Kaler, K. E. Bennett, H. T. Davis, and L. E. Scriven, J. Chem. Phys. **79**, 5673, 5685 (1983); N. J. Chang and E. W. Kaler, *ibid.* (in press).

[8]A. M. Cazabat, D. Langevin, J. Meunier, and A. Pouchelon, J. Adv. Colloid Interface Sci. **16**, 175 (1982).

[9]P. Ekwald, in *Advances in Liquid Crystals I*, edited by G. H. Brown (Academic, New York, 1975), p. 1; A. M. Bellocq and D. Roux, in *Microemulsions*, edited by S. Friberg and P. Bothorel (Chemical Rubber, New York, 1986); D. H. Smith, J. Colloid Interface Sci. **102**, 435 (1984).

[10]K. Shinoda and H. Saito, J. Colloid Interface Sci. **26**, 70 (1968); M. L. Robbins, in *Micellization, Solubilization, and Microemulsions*, edited by K. Mittal (Plenum, New York, 1977), p. 713.

[11]The terminology upper, lower, and middle arises from the position occupied by the microemulsion in the test tube.

[12]L. A. Turkevich and S. A. Safran, in Ref. 1(a).

[13]H. Saito and K. Shinoda, J. Colloid Interface Sci. **32**, 647 (1970); D. Guest and D. Langevin, *ibid.* **112**, 208 (1986); E. Ruckenstein and J. Chi, J. Chem. Soc. Faraday Trans. 2 **71**, 1690 (1975).

[14]See, *Surface Phenomena in Enhanced Oil Recovery*, edited by D. O. Shah (Plenum, New York, 1981); *Proceedings of SPE/DOE Fifth Symposium on Enhanced Oil Recovery*, April 1986 (Society of Petroleum Engineering, New York, 1986), Vols. 1–2.

[15]See the experimental papers in Ref. 1.

[16]P. G. de Gennes and C. Taupin, J. Phys. Chem. **86**, 2294 (1982).

[17]J. Jouffroy, P. Levinson, and P. G. de Gennes, J. Phys. (Paris) **43**, 1241 (1982).

[18]B. Widom, J. Chem. Phys. **81**, 1030 (1984).

[19]G. L. Gaines, *Insoluble Monolayers at Liquid–Gas Interfaces* (Wiley, New York, 1966).

[20]J. C. Wheeler and B. Widom, J. Am. Chem. Soc. **90**, 3064 (1968).

[21]B. Widom, J. Chem. Phys. **84**, 6943 (1986).

[22]M. Schick and W. H. Shih, Phys. Rev. B **34**, 1797 (1986); K. Chen, C. Ebner, C. Jayaprakash, and R. Pandit, J. Phys. C **20**, L361 (1987).

[23]Despite this large correlation length, the system is not in general near any kind of critical point. Under these conditions, it is a difficult mathematical task to extract the relevant behavior from a microscopic Hamiltonian.

[24]Also, it may be difficult to eliminate spurious effects arising from the lattice construction. For example, it is difficult to count bending energies correctly with a local Hamiltonian, operating on discrete spin-like variables. The bending energy of a surfactant-covered spherical globule of oil is independent of its size R. On a cubic lattice, however, the corresponding state of lowest bending energy is a cube, which has a bending energy proportional to R/a, with a being the lattice spacing. One way to eliminate this kind of discrepancy is to choose the lattice spacing to be of the same order as the domain size R. This is, however, tantamount to taking the phenomenological approach.

[25]Experiments have shown that the area per head is approximately constant along the two-phase coexistence curves—see Ref. 6.

[26]S. A. Safran, D. Roux, M. Cates, and D. Andelman, Phys. Rev. Lett. **57**, 491 (1986); *Surfactants in Solution: Modern Aspects*, edited by K. Mittal (Plenum, New York, in press).

[27]W. Helfrich, J. Phys. (Paris) **46**, 1263 (1985); **48**, 285 (1987).

[28]L. Peliti and S. Leibler, Phys. Rev. Lett. **54**, 1690 (1985).

[29]D. Forster, Phys. Lett. A **114**, 115 (1986); W. Kleinert, *ibid.* **114**, 263 (1986).

[30]In the absence of the renormalization of the bending constant, the phase diagram still shows a three-phase equilibrium, similar to that of Ref. 18. However, the length scale of the microemulsion in the middle phase is unrelated to the properties of the surfactant film (e.g., the persistence length). In addition, the free energy is greater than that of a lamellar phase.

[31]J. M. di Meglio, M. Dvolaitzky, and C. Taupin, J. Phys. Chem. **89**, 871 (1985).

[32]This is also the minimum amount of surfactant needed to obtain a one-phase microemulsion with the same amount of water and oil, within our model.

[33]This critical point is in fact a tricritical point whose nature is the same as the tricritical points of Widom's model (see Ref. 18).

[34]This is true for micellar phases where the globules are compact.

[35]Since $\chi_w > 0$, a concentrated micellar phase where the entropy is negligible is itself unstable and would probably coexist with a lamellar phase which does not have the energy penalty of curved surfactant layers.

[36]There is a window in the values of χ_0 or χ_w where the middle-phase region is stable. In order for the minima in the dilute regime to be narrow, χ_0 or χ_w must be large. If χ_0 or χ_w is not large enough, the three phases which coexist consist of three microemulsion phases, and not a microemulsion in equilibrium with nearly pure water and oil. However, if χ_0 or χ_w is too large, the minima are not deep enough and the two-phase coexistence dominates.

[37]W. Helfrich, Z. Naturforsch. Teil A **28**, 693 (1973); **33**, 305 (1978). See also, D. Roux and C. Coulon, J. Phys. (Paris) **47**, 1257 (1986).

[38]C. Safinya, D. Roux, G. S. Smith, S. K. Sinha, P. Dimon, N. A. Clark, and A. M. Bellocq, Phys. Rev. Lett. **37**, 2718 (1986).

[39]The steric repulsion is not relevant for our model of the middle phase at length scales smaller than the lattice size ξ. This is because the steric repulsion applies only to two surfaces whose size is much larger than their spacing [see D. Sornette and N. Ostrowsky, J. Phys. (Paris) **45**, 265 (1984)]. At length scales greater than the lattice spacing, the self-avoidance of the surfactant film is accounted for by the lattice construction.

[40]D. H. Smith, J. Colloid Interface Sci. **102**, 435 (1984). For a review see Ref. 1.

[41]Other changes involve discrete changes in the type of surfactant, hydrophile and lipophile size, number of carbon double bonds, aromaticity of the oil, etc.